ORIGINAL PAPER

On the Application of Transition State Theory to Atomic-Scale Wear

Tevis D. B. Jacobs · Bernd Gotsmann ·
Mark A. Lantz · Robert W. Carpick

Abstract The atomic force microscope (AFM) tip is often used as a model of a single sliding asperity in order to study nanotribological phenomena including friction, adhesion, and wear. In particular, recent work has demonstrated a wear regime in which surface modification appears to occur in an atom-by-atom fashion. Several authors have modeled this atomic-scale wear behavior as a thermally activated bond breaking process. The present article reviews this body of work in light of concepts from formal transition state theory (also called *reaction rate theory*). It is found that this framework is viable as one possible description of atomic-scale wear, with impressive agreements to experimental trends found. However, further experimental work is required to fully validate this approach. It is also found that, while the Arrhenius-type equations have been widely used, there is insufficient discussion of or agreement on the specific atomic-scale reaction that is thermally activated, or its dependence on stresses and sliding velocity. Further, lacking a clear picture of the underlying mechanism, a consensus on how to measure or interpret the activation volume and activation energy is yet to emerge. This article makes suggestions for measuring and interpreting such parameters, and provides a picture of one possible thermally activated transition (in its initial, activated, and final states). Finally, directions for further experimental and simulation work are proposed for validating and extending this model and rationally interrogating the behavior of this type of wear.

Keywords Nanotribology · Contact mechanics · AFM · Unlubricated wear · Wear mechanisms

T. D. B. Jacobs
Department of Materials Science and Engineering, University of Pennsylvania, 220 S. 33rd St., Philadelphia, PA 19104, USA
e-mail: tevis@seas.upenn.edu

B. Gotsmann · M. A. Lantz
IBM Research, Zurich, Saeumerstrasse 4, 8803 Rueschlikon, Switzerland

R. W. Carpick (✉)
Department of Mechanical Engineering and Applied Mechanics, University of Pennsylvania, 220 S. 33rd St., Philadelphia, PA 19104, USA
e-mail: carpick@seas.upenn.edu

1 Introduction

With the advent of nanotechnology over the last decade, it has become necessary to gain a fundamental understanding of wear at the nanometer and atomic scales. As device length scales shrink and surface-to-volume ratios grow, adhesive and frictional forces become increasingly important. Already, microelectromechanical systems (MEMS) with gears or other sliding contacts demonstrate unacceptably low lifetimes due to wear; such issues are exacerbated as dimensions shrink into the nanometer scale [1–3]. Nanoscale wear is also critical for tip-based nanomanufacturing (TBN) applications, where a nanoscale tip (or array of tips) in a scanning probe microscope (SPM) is used to locally deposit, modify, or manipulate material at the nanometer or the atomic scale [4–7]. A fundamental scientific and technological challenge involves understanding and maintaining the structural and chemical integrity of the tip.

The atomic force microscope (AFM) has become a standard tool for studying nanoscale contact phenomena by sliding a single asperity across a well-defined surface

[8, 9]. Recently, a number of experimental studies have used AFM to characterize wear progression for a variety of material systems under various loads, velocities, and environments [10–21]. Much of this recent work has shown that Archard's law—which states that the worn volume is proportional to sliding distance and applied load, and independent of sliding velocity or apparent contact area—is inadequate for describing wear in nanoscale single asperity sliding contacts [22]. For example, the wear rate, defined as wear volume per unit normal force and sliding distance, is typically not constant for single asperities sliding on surfaces [13, 15, 20, 22]. In addition, the nanoscale wear rates do not appear to be independent of velocity [15, 23]. Finally, a non-linear dependence of wear rate on applied load has been observed for both single asperity wear (i.e., tip wear) and surface wear [24]. As a consequence, new models have been put forth to explain the progression of wear in these experiments [12, 14, 22, 25].

Recently, experimentation has allowed the observation of wear rates sufficiently small to propose that atom-by-atom wear is occurring [22, 26, 27]. In other words, the surface modification is occurring by the removal of individual atoms or small clusters of atoms rather than by larger-scale modification such as fracture or plastic deformation. The evidence for this behavior is as follows: the rate of wear in this regime is ultra low—in some cases calculated to be as low as one atom per millimeter of sliding [22]; also, there has been crystalline structure observed in the redeposited wear debris [26] (indicating small enough debris particles that reordering is possible); and finally the smoothness of the profiles of worn probes indicates a nano-scale unit of wear events. A recent example of this gradual evolution of a scanning probe is shown in the work of Liu et al., where transmission electron microscopy (TEM) imaging is used to periodically measure the profile of an AFM probe at various scan distances [28]. Figure 1 contains traced profiles of a silicon nitride tip at five different scan distances and shows the gradual, progressive modification of the probe surface. The models that have been proposed to describe wear in this regime [13, 14, 22] use formalisms developed for thermally activated processes (for example, atomic diffusion in a crystal lattice).

The purpose of this article is to review the current state of this type of wear modeling and to pose relevant questions and suggestions for future study to the tribology community. Section 2 of this article briefly reviews the basic principles of formal transition state theory, including an example where it has been fruitfully used: temperature-dependent plastic flow by dislocation glide. Section 3 reviews recent literature in which experimental wear results have been analyzed in the context of transition state theory and then discusses common themes and open
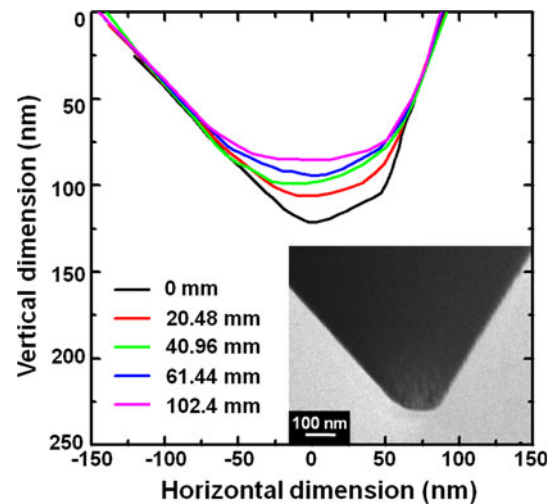
Fig. 1 Traced profiles of silicon nitride atomic force microscope probe demonstrating the gradual wearing away of the probe surface. Traces are extracted from TEM images (an example of which is shown in the inset), taken periodically during AFM scanning against a polycrystalline diamond surface. (The total distance scanned for each profile is indicated in the figure legend.) Figure adapted from [70]

questions. Finally, Sect. 4 proposes future work to be done in this area—including suggested experimental work to further interrogate the thermal activation model and suggested modifications to the latest wear models.

2 Brief Overview of Transition State Theory and Some Applications

Transition state theory (also called *absolute rate theory* or *reaction rate theory*) originated as a framework for describing the kinetics of thermally activated chemical reactions. The classic formulation describes a set of reactants that undergo a process which moves them from one stable equilibrium point (the initial state) to another (the final state). The degree of progress is measured as the *reaction coordinate*. Stable equilibrium demands that the two terminal points lie at local energy minima and therefore at least one local maximum must exist at an intermediate position along the reaction coordinate. In the simplest picture, shown in Fig. 2, there is one maximum and the state of the system at this point is called the *activated complex*. The energy difference between the initial and activated states is known as the *activation energy* (ΔG_{act}). For a large number of identical systems, Eyring used statistical mechanics to describe the overall rate of forward reaction k for a thermally activated process [29]:

$$k = f \exp\left(-\frac{\Delta G_{\mathrm{act}}}{k_{\mathrm{B}} T}\right), \tag{1}$$
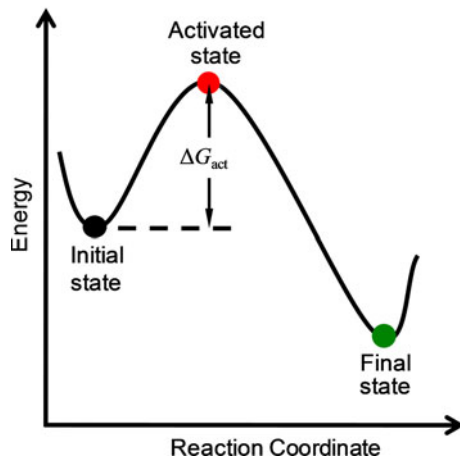
Fig. 2 Schematic diagram showing the energy as a function of reaction coordinate for a system as it undergoes a thermally activated process. Figure adapted from [29]

where f is an effective attempt frequency, ΔG_{act} is the Gibbs free energy of activation, k_B is the Boltzmann constant, and T is the absolute temperature.

There are five assumptions inherent in his analysis [29]: (1) there is a continuous change along the reaction coordinate linking the stable initial and final states and the intermediate, unstable activated state; (2) the reaction will proceed along the lowest-energy path, thus the activated state will lie at a saddle point in energy; (3) once the system has reached the activated state, there is a high probability that it will proceed to the final state; (4) the initial state and activated state are at thermal equilibrium, such that Boltzmann statistics can be applied; and (5) the activated state possesses all degrees of freedom *except* vibrational motion along the reaction coordinate (which causes decomposition to the initial or final states). The last assumption indicates that even the activated state is a point of stable equilibrium with respect to all other variables—it is only in the reaction coordinate that there is an energy maximum.

While this rigorous theoretical basis applies well to chemical reactions, its extension to solids is more complex as a crystal of N atoms contains $3N$ degrees of freedom and therefore the potential energy landscape is a $3N$-dimensional hypervolume. Vineyard was able to formulate the general, many-body problem and solve it rigorously in the context of reaction rate theory by approximating system vibrations as harmonic [30]. His treatment described chemical diffusion by atomic hops. In the absence of an external force, there is no work done on or by the system; therefore Vineyard used the Helmholtz free energy of activation $\Delta F_{act} = \Delta U_{act} - T\Delta S_{act}$, where ΔU_{act} and ΔS_{act} are the differences in potential energy and entropy, respectively, between the initial and activated states (the

activation energy and *activation entropy*). By describing the potential energy landscapes around the initial and activated states as those of simple harmonic oscillators, the following Arrhenius-type rate equation can be derived [30]:

$$k = f \exp\left(-\frac{\Delta F_{act}}{k_B T}\right) = \left\{\frac{\prod\limits_{j=1}^{3N} f_j}{\prod\limits_{j=1}^{3N-1} f_j'}\right\} \exp\left(-\frac{\Delta U_{act}}{k_B T}\right), \qquad (2)$$

where f is an effective vibration frequency, and f_j and f_j' are the normal frequencies of oscillation about the initial state and the activated state in each of j degrees of freedom. In accordance with assumption (5) of the Eyring treatment, the system has the full $3N$ degrees of freedom at its initial state, but only $3N - 1$ at the activated state since, in that state, any vibration along the reaction coordinate causes decomposition to one of the terminal states. In many cases, the effective frequency factor is assumed to be in the range of 10^{12}–10^{13} Hz based on either of two assumptions: the vibrational modes of the initial and activated state can be assumed very similar such that the pre-factor shown in curly braces in Eq. 2 simplifies to the vibration frequency at the well bottom (Eq. 3.5 in [31]); alternatively, with appropriate substitution for the partition functions of the activated and initial states and under the assumption of negligible reactive volume, it can be shown that the other pre-factor takes the form $f = k_B T/h$, which is equal to $6.2 * 10^{12}$ Hz at room temperature (Eq. 3.19 in [31]).

2.1 Case Study on Transition State Theory: Plastic Flow by Dislocation Glide

In the 1950s and 1960s, substantial research was dedicated to the plastic flow of crystalline metals in which deformation occurs by the motion of line defects (*dislocations*), which facilitates the relative motion of adjacent planes of atoms. Experimentally, many studies (such as [32, 33]) demonstrated a logarithmic dependence of both strain rate (the time rate of change of the strain of the crystal) and dislocation velocity on the applied shear stress and on the inverse temperature. This behavior was explained using the formalism of transition state theory.

Articles by Gibbs [34], Hirth and Nix [35], and others describe a detailed model whereby the macroscopic behavior was characterized as the aggregate of a very large number dislocations, each of which has its motion pinned at various points by obstacles (such as crystal defects). In the initial state, the local dislocation segments are in mechanical equilibrium due to the opposing forces of the external applied stress and the local resistance to motion, which is increased by the obstacle, as shown in Fig. 3a. The mechanical energy provided by the applied stress is
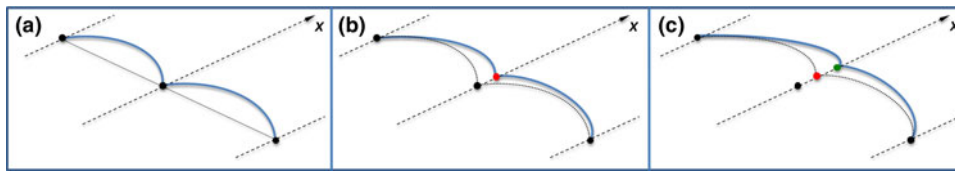
Fig. 3 Schematic model showing a perspective view onto a plane where a dislocation segment (*thicker, solid line (blue)*) is undergoing thermally activated advancement. In the initial state (shown in **a**), the dislocation is in stable equilibrium and bows outward between pinning points. The *black dots* represent stable equilibrium points along the reaction coordinate (which is a spatial axis designated, for the central pinning point, by *x*); the *dots* do not represent the obstacles themselves. In (**b**), the central region of the dislocation has accessed the activated state (designated by a second *dot (red)* located further along the reaction coordinate). In (**c**), this section of the dislocation has advanced to a new stable equilibrium point (designated by a third *dot (green)* located still further along *x*); the motion of the dislocation is now impeded by some other obstacle. Figure adapted from [35]. (Color figure online)

insufficient to overcome the energy barriers represented by the pinning points. Therefore, the system must rely on thermal fluctuations to allow the dislocation segments to reach the unstable activated state (Fig. 3b), where the forces *just* balance and any perturbation causes decomposition either back into the initial state or forward into the final state. In the final state (Fig. 3c), the dislocation has reached a new stable equilibrium state due to some other obstacle. All activation parameters describe the transition between the initial and activated states.

For a very large number of these pinned dislocations, Boltzmann statistics apply and the process can be modeled with an analysis similar to that of Vineyard's. In this picture, work is done during the transition and therefore the Gibbs free energy of activation ($\Delta G_{act} = \Delta H_{act} - T\Delta S_{act}$) is used, where the activation enthalpy is $\Delta H_{act} = \Delta U_{act} - \Delta W_{act}$ and ΔW_{act} is the work done during the transition from initial to activated state [36]. In this formulation, the overall strain rate $\dot{\varepsilon}$ can be described with an Arrhenius form [37]:

$$\dot{\varepsilon} = \dot{\varepsilon}_0 \exp\left(-\frac{\Delta G_{act}}{k_B T}\right), \tag{3}$$

where $\dot{\varepsilon}_0$ is an appropriate pre-exponential factor. Therefore, using thermodynamics and rearranging Eq. 3, the rigorous definitions of activation volume ΔV_{act} and activation enthalpy can be determined as follows [34, 37]:

$$\Delta V_{act} = -\left(\frac{\partial \Delta G}{\partial \sigma^*}\right)_T = -k_B T \left(\frac{\partial \ln(\dot{\varepsilon}/\dot{\varepsilon}_0)}{\partial \sigma^*}\right)_T, \tag{4}$$

$$\Delta H_{act} = -\left(\frac{\partial (\Delta G/T)}{\partial (1/T)}\right)_{\sigma^*} = k_B T^2 \left(\frac{\partial \ln(\dot{\varepsilon}/\dot{\varepsilon}_0)}{\partial T}\right)_{\sigma^*}, \tag{5}$$

where σ^* is the resolved shear stress acting on the dislocation. It is important to note that the activation volume does not by definition describe an actual physical volume, but, as will be discussed later, it is sometimes associated with one.

In principle, these quantities should be directly measurable by experiment. In practice, it remains difficult to

interpret experimentally measured values of activation volume and enthalpy, as is clearly elucidated by Hirth and Nix [35]. The first problem comprises the accurate determination of the stress. The exact state of stress acting at the local area where the reaction is taking place is often complex and difficult to accurately specify. In addition, the measured, macroscopic rate involves the action of many microscopic processes, which may not all experience the same state of stress. Second, the stress acting locally may change over the course of a test, even if the macroscopic applied stress is constant. Third, the pre-exponential factor ($\dot{\varepsilon}_0$ in Eq. 3) cannot be measured independently, so it must be assumed constant with respect to stress and temperature. Finally, at low stress levels, the reverse dislocation jump rate is no longer negligible and the rate equation needs to be modified to include a reverse term. As will be shown, each of these difficulties has an analog in the analysis of atomic-scale wear.

Despite all of these difficulties, measured values are useful as a signature for a given process and have been fruitfully compared across different experiments with significant success. In many cases, they can even be related to physical quantities. For example, the work done ΔW_{act} is often further defined as $\sigma^* b \Delta A_{act}$, where b is the Burgers vector of the dislocation and ΔA_{act} is the area swept out by the dislocation as it moves from the initial to the activated state [36, 38]. This relation allows the dislocation behavior to be associated with the distribution of obstacles, enabling understanding and prediction of the behavior of materials undergoing plastic flow.

However, dislocation-mediated plastic flow also provides examples where reaction rate theory *cannot* be applied. For instance, dislocation motion is opposed not only by the short range forces described above, but also by long range forces such as elastic interactions with other dislocations [39]. The energy barriers from the latter forces can be too large to be overcome by thermal activation. Therefore, the thermally activated description will only apply up to some critical temperature, where the flow stress reaches the *athermal limit*. As temperature increases

further, the flow stress will continue to decrease, but now due to the variation of shear modulus G with temperature. Thermal softening is an entirely different effect and any attempts to model flow stress in this regime using a thermally activated model would yield meaningless values of activation parameters. There are countless examples of other processes, some of which might even be highly temperature-dependent, where the macroscopic behavior is *not* described by an aggregate of a large number of local processes, where the energy barrier is too small (relative to $k_B T$) for Boltzmann statistics to apply, or where for some other reason the formalism of transition state theory cannot be applied.

Reviewing the well-established literature on thermally activated plastic flow provides useful insights, which will be applied in the following sections to the developing theory of thermally activated atomic-scale wear. In particular, the above example demonstrates the usefulness of a clear description of the microscopic mechanism underlying the larger behavior, including a picture of the transitioning system in its initial and activated states. The example also demonstrates the challenges of analyzing the model and interpreting experimentally measured parameters.

3 Atomic-Scale Wear Analyzed in the Context of Transition State Theory

In recent years, transition state theory has been developed to apply to atomic-scale wear. In particular, Park et al. [40], Sheehan [41], Gotsmann and Lantz [22], and Bhaskaran et al. [27] experimentally measured wear of nanoscale contacts and analyzed the results using an Arrhenius analysis. The analysis of all four papers is built on the

assumption that the fundamental rate of atom loss (atoms removed per second) due to wear can be described as:

$$k_{\text{atom-loss}} = k_0 \exp\left(-\frac{\Delta G_{\text{act}}}{k_B T}\right), \tag{6}$$

where k_0 is some pre-factor analogous to $\dot{\varepsilon}_0$ in plastic flow. The following section probes the analysis and assumptions of this approach in light of the discussion in Sect. 2.

3.1 Recent Studies of Atomic-Scale Wear as a Thermally Activated Process

In an early study by Park et al., a silicon nitride probe tip was raster-scanned across a dissolving surface step of calcite in a saturated aqueous environment [40]. Scanning increased the rate of dissolution of ions at the step edge. Simultaneous topographic images showed that double kinks nucleated on the step edge and grew laterally such that the step receded by one lattice spacing a per dissolution (or wear) event. Thus, the rate of wear track growth, V_{track} (the distance the step recedes in nanometers per second), is proportional to the time-rate of wear, $k_{\text{atom-loss}}$. When the rate V_{track} is plotted against the applied normal contact force F_N, there is an exponential dependence, as shown in Fig. 4a. The authors model this behavior using Arrhenius kinetics and transition state theory.

The authors assume a form for the work done during the transition as $\Delta W_{\text{act}} = \sigma_{\text{rr}} \Delta V_{\text{act}}$, where σ_{rr} refers to the radial contact stress predicted by Hertzian contact mechanics at the points where this stress achieves its largest tensile value, which occurs right at the edge of the contact zone (Fig. 5) on the surface. All of the stress components in the Hertzian picture scale with the mean contact pressure, which is given by $p_m = \frac{1}{\pi}(F_N K^2 / r^2)^{1/3}$,
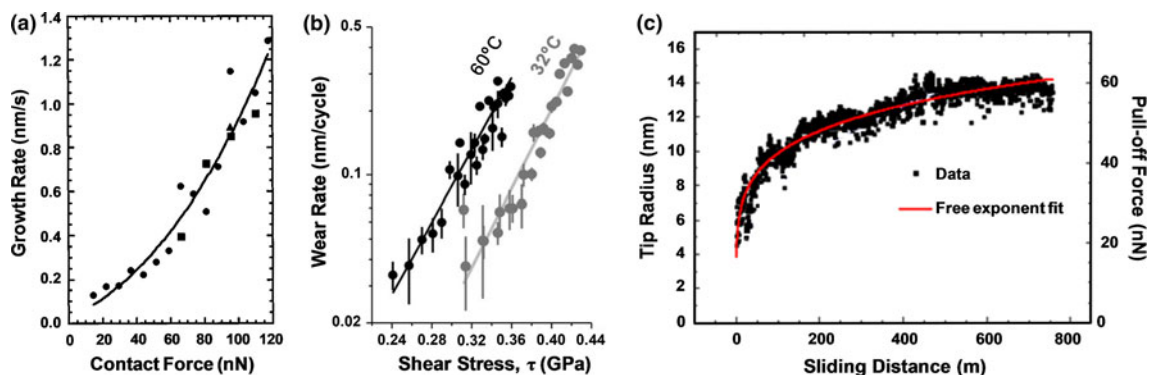

Fig. 4 Charts showing the experimental results from various wear studies. The wear track growth rate (shown to be proportional to the wear rate) from Park [40] (**a**), and the calculated wear rate from Sheehan [41] (**b**) both show the exponential growth with increasing load or stress. The evolution of tip radius from Gotsmann [22] (**c**) is shown as a function of sliding distance. The decreasing rate of change of tip radius is explained by the decreasing surface stresses as the load

stays constant and the tip gets blunter. In all three studies, the *solid line* represents a model of the experimental behavior based on transition state theory. Figures reprinted with permission from: [40] (**a**); [41] (**b**); and [22] (**c**)—Copyright 1996, American Institute of Physics; 2005, Elsevier; and 2008, American Physical Society, respectively
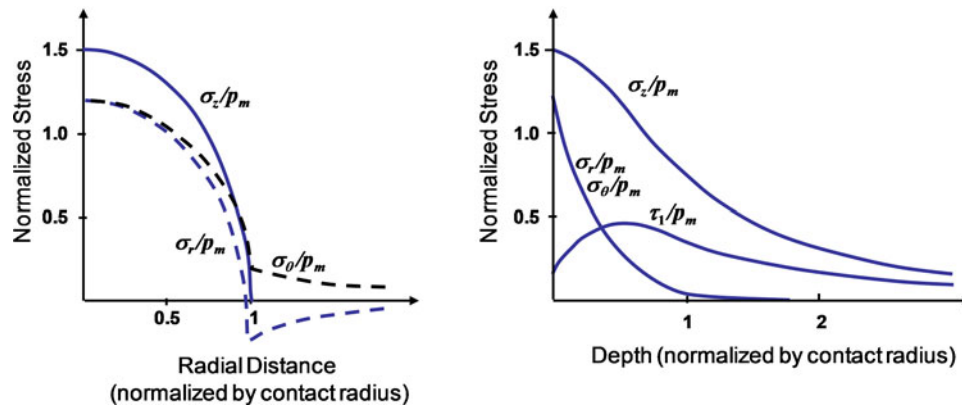
Fig. 5 Stress distributions for the radial (σ_r), circumferential (σ_θ), and normal stresses (σ_z) normalized by the mean contact pressure (p_m) for the Hertz contact model. The contact radius is a. The surface stresses are shown at left as a function of the radial coordinate r with compressive stress drawn positive, tensile stress negative. The plot at right shows the variation of stresses with depth z/a into the body. The maximum in-plane shear stress (τ_1) is indicated with a *dashed line* at right. Figure adapted from [54]

where r is the radius of the tip, and $K = 4/3 \left[(1 - v_1)^2/E_1 + (1 - v_2)^2/E_2 \right]^{-1}$, where E_1, E_2 are the Young's moduli of the tip and sample, and v_1, v_2 are Poisson's ratios of the tip and sample, respectively. Using these assumptions, the rate of wear track growth can be written as:

$$
\begin{aligned}
V_{\text{track}} &= ak_{\text{atom−loss}} = ak_0 \exp\left(-\frac{\Delta G_{\text{act}}}{k_B T} \right) \\
&= ak_0 \exp\left(-\frac{\Delta U_{\text{act}} - \Delta V_{\text{act}} \sigma_{rr}}{k_B T} \right).
\end{aligned} \tag{7}
$$

In this picture, V_{track} varies exponentially with changes in the stress and, by fitting the experimental data, an activation volume can be directly extracted. Since temperature was not varied, the activation enthalpy cannot be directly measured. Instead, the authors estimate values for all non-measurable quantities in Eq. 7 and then solve the equation for ΔU_{act}. This approach for calculating the activation energy is less direct and will have larger uncertainty, as discussed later in this section, but it does enable an estimate of the activation energy. The results are shown in Table 1.

Similar experiments were performed by Sheehan on NaCl in N_2 environments at different relative humidities and at two different temperatures [41] (32 and 60 °C) (Fig. 4b). This work reported similar behavior to that of Park et al. [40], and was analyzed using equations similar to (7) above. Instead of using the Hertzian radial stress (which, as stated above, corresponds to the largest tensile stress, at the edge of the contact zone), Sheehan proposed that the shear stress would have the most significant effect on atomic-scale wear. As shown in Fig. 5, this stress is not largest at the surface, but rather at a depth equal to roughly half the contact radius. As with the Park study, the

measurements of wear rate versus stress are fitted and a value for the activation volume is extracted from the best-fit curve (Table 1). By introducing temperature variation, Sheehan's data is the first to measure changes in wear rate with temperature and thus is the first set of data where the activation enthalpy could be directly accessed (as described in Eq. 5). However, having only two temperature data points over a limited temperature range leads to rather large uncertainty in this value.

Gotsmann and Lantz applied Arrhenius kinetics to the wear of the scanning tip rather than the scanned surface [22]. In this investigation, the radius change of silicon probe tips was monitored in situ during extremely long-distance scanning at a variety of applied loads over a polymer (polyaryletherketone) surface. Sharp, conical tips with initial radii of 3–5 nm were scanned for hundreds of meters. An in situ force–displacement test was performed at regular intervals to measure pull-off force $F_{\text{pull-off}}$, which was used to calculate the tip radius. During sliding, the tip radius changes as shown in Fig. 4c. The rate of atom loss from the tip is modeled using Eq. 6, then assumptions about the tip shape are used to determine the rate of change of the flattened tip radius r. By further assuming a form for the shear stress τ adapted from the work of Briscoe and Evans [42], the authors model the change in radius with sliding distance d as:

$$
\frac{dr(d)}{dd} = \tan(\theta)\left(\frac{bk_0}{v_0} \right) \exp\left(-\frac{\Delta U_{\text{act}}}{k_B T} + \frac{\Delta V_{\text{act}}}{k_B T}[\tau_0 + \xi P] \right),
\tag{8}
$$

where ξ is the pressure dependence of shear stress, τ_0 is the value of the shear stress extrapolated to zero pressure, and v_0 is a characteristic velocity (the values chosen for these parameters are discussed later). P denotes the pressure under the tip calculated using $P = (F_N + k_{\text{adh}}r)/(\pi r^2)$. F_N

Table 1 The experimentally determined values of activation energy and volume for four atomic-scale wear studies

System	Activation energy	Activation volume
Nanoscale wear experiments		
Atomic-scale wear of calcite sample [40]	0.80 ± 0.2 eV (calculated)	37 ± 3 Å^3
Atomic scale wear of NaCl sample [41]	0.34 ± 0.17 eV (measured)	86 ± 6 Å^3
Atomic scale wear of Si tips [22]	0.98 ± 0.04 eV (calculated)	55 ± 35 Å^3 (110 Å^3)^a
Atomic scale wear of silicon-oxide containing DLC tips [27]	1.0 ± 0.1 eV (calculated)	340 ± 200 Å^3
(Typical values for other thermally activated processes)		
Dislocation nucleation (forest) in bulk		100–1,000 b^3
Dislocation nucleation at surfaces [68]	0.1–0.6 eV	1–10 b^3
Atomic vacancy creation (Schottky defect) [69]	0.1–7 eV	
Atomic vacancy hopping [48]	0.05–0.5 eV	0.02–0.2 b^3

Values are also presented for several other processes that are known to be thermally activated. Activation volumes are typically given in units of the Burgers vector that is typically 2.5–6 Å, and therefore $b^3 \sim 10$–200 Å^3. The ranges of numbers given are for very different materials and typically scale with the degree of covalent bonding between neighboring atoms

^{a} Assuming $\xi \sim 0.5$ (Cannara R, Gotsmann B, Lantz MA, Unpublished results 2007)

is the applied load and k_{adh} is a constant defined by the adhesive load $F_{adh} = k_{adh} * r$.

Equation 8 is numerically solved for r and fit to the experimental tip wear data using an effective activation energy ($\Delta U_{act} - \Delta V_{act} \ \tau_0$) and an effective activation volume ($\xi \Delta V_{act}$) as fitting parameters. Note that while the rate of wear exhibits the familiar exponential dependence on stress in this model, the shape of the curve in Fig. 3c reflects the fact that the contact stresses change as wear progresses and the tip gets blunter. Bhaskaran et al. used the same model to analyze data from a related study of a silicon-oxide containing diamond like carbon (DLC) tip over a silica surface [27]. The results from both studies are included in Table 1.

While the many difficulties of accurately extracting and interpreting values of experimentally measured parameters will be discussed below, it is interesting to compare values as they are reported in the various studies, as shown in Table 1. First of all, the order of magnitude of all measured parameters is consistent with a highly localized activation reaction involving a small number of atoms and the rupture of a small number of bonds. Second, the reported activation energies for wear of the covalently bonded solids (silicon and silicon-oxide containing DLC probes) are quite similar in the range of 1 eV, while energies of the ionically bonded solids (sodium chloride and calcite) are lower. It should be noted that due to the form of the shear stress, the model used in the Gotsmann and Lantz study only allows effective activation parameters to be extracted since, mathematically, the *effective* activation barrier $\Delta U_{act} - \tau_0 \Delta V_{act}$ and the *effective* activation energy $\xi \Delta V_{act}$ cannot be further broken down. Through separate studies of the pressure-dependence of velocity, the authors were able to measure $\xi = 0.5$ for a silicon probe on polyaryletherketone (Cannara R, Gotsmann B, Lantz MA, Unpublished results,

2007), therefore an effective activation volume of 55 Å^3 corresponds to an activation volume of 110 Å^3. For reference, typical values of activation parameters for some other common thermally activated processes are included in Table 1. As mentioned, the measured values for a thermally activated picture of wear are consistent with the order of magnitude of these other highly localized processes.

Additional thermally activated models of atomic-scale wear have been proposed, though other studies did not directly measure or calculate values for activation parameters. Kopta and Salmeron examined wear of muscovite mica samples during AFM scanning in humid air [24]. Specifically, the authors observed that 2 Å-deep wear scars appeared in the mica after a certain number of scans, indicating detachment of the top layer of SiO_4 tetrahedra. Significantly, wear pits only developed after a characteristic number of scans, which depended on the total applied load F_N. The authors modeled this behavior as thermally activated cleavage of Si–O bonds, detaching single SiO_4 tetrahedra and leaving behind point defects not observable in the AFM images. When the density of defects reaches a critical level, a large section of the top layer detaches, creating a detectable wear pit. The authors are able to accurately fit their data using an exponential equation derived from transition state theory. However, the authors did not directly calculate the activation parameters. Their description of wear progression in mica (individual bond scission events leading to larger-scale displacement of mica layers) was later validated using lattice-resolved friction images of the evolving mica surface [43]. The latter authors also investigate the effect of solution pH on wear progression and find that the activation barrier for acid-catalyzed bond breaking is significantly higher than for base-catalyzed reaction.

A theoretical model of thermally activated sample wear has been developed by D'Acunto, in which the transitioning atoms undergo a diffusion-like hopping process [14]. This model considers wear of sample atoms in two ways: (1) the atom can be pulled onto the tip due to Van der Waals attraction, or (2) it can be dragged along the surface by shear forces. In this model, the two processes are modeled using Arrhenius rate laws with independent activation barriers. This model usefully considers the question of what happens to the atoms after they are worn away, which is not considered in the other models. The barrier for jumping between the tip and sample is taken as the attractive term in the equation for the van der Waals force, and is thus dependent on tip/sample separation. The barrier for jumping laterally is taken as the height of the corrugations of the sample's potential energy surface. According to the assumptions in the article, the barrier for lateral jumps is significantly lower and therefore this is taken as the primary wear mechanism. While this model is also based on an Arrhenius rate law, results cannot be compared directly with the Park, Sheehan, or Gotsmann models since the activation barrier (taken as the energy surface corrugation) is independent of normal or frictional forces.

3.2 Expanding on the Model of Atomic-Scale Wear as a Thermally Activated Process

While a transition state analysis does appear to fit the data quite accurately for the different types of wear studies mentioned, it is still important to ask the question of whether a thermally activated model can be meaningfully applied. The primary test for whether a process obeys Boltzmann statistics, and thus can be considered thermally activated, is a study of the variation in the rate of the process with temperature. Such studies have been conclusively carried out for plastic flow, as discussed in Sect. 1. This temperature dependence has not yet been demonstrated for atomic-scale wear, though there has been some

experimental work showing Arrhenius behavior of *macroscale* wear [44]. While the one atomic-scale study where temperature was varied [41] was consistent with a thermally activated process, only two similar temperatures could be accessed experimentally. There has not yet been a systematic study examining atomic-scale wear over a wide range of temperatures. The thermally activated formalism provides one potentially powerful way to analyze the data. However, without experimental demonstration of the temperature dependence, it must be applied with caution.

Further, if atomic-scale wear is a thermally activated process, one must describe the specific atomic-scale mechanism by which it progresses, including a picture of the system in its initial, activated, and final states. The aforementioned studies implicitly propose that the underlying local process is one of atom-by-atom attrition, analogous to dissolution or desorption of atoms from a surface. This is appealing since dissolution and desorption are commonly modeled as thermally activated processes and it is intuitively reasonable to model atomic-scale wear as a stress-assisted version of the same mechanism. It would be useful to take this one step further by creating a schematic picture similar to that shown in Fig. 3. A prototypical example of such a model is shown and described in Fig. 6. Having this type of picture allows a more concrete interpretation of the activation parameters. For example, in the model shown in Fig. 6, the activation parameters describe *only* the transition from the adjacent equilibrium states shown in Fig. 6b, c. Thus, in this picture, the activation barrier is *not* equivalent to the vacancy formation energy (the energy change in going directly from state (a) to state (e)) as these are not adjacent equilibrium states.

The set of schematic pictures in Fig. 6 is included primarily as a prototypical example of how to concretely specify the underlying thermally activated reaction and the configuration of the system in its initial, activated, and final states. It is meant to demonstrate the utility of having such a picture and is not proposed as a complete picture of the wear process.
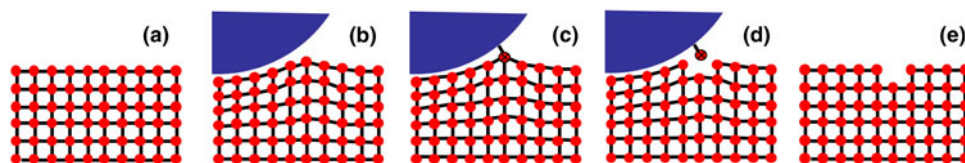

Fig. 6 A schematic atomic-scale model of one possible thermally activated mechanism by which wear of a substrate occurs. The unperturbed surface (**a**) is brought into quasi-static equilibrium with the sliding tip, as shown in (**b**). In (**c**), a single atom (marked with an x) is in an unstable equilibrium state—mid-way along its transition from being sample-bonded (as it is in **b**) to being tip-bonded (as it is in **d**). In (**e**), the elastic deformation has been relaxed (and any surface

reconstruction has occurred (not shown), leaving a worn surface behind. In the language of transition state theory, state (**b**) represents the initial state, (**c**) represents the activated state and (**d**) represents the final state. All activation parameters would describe the transition from (**b**) to (**c**). It is further required that the change in free energy between (**c**) and (**d**) is significant, so that the reverse process is not likely

3.3 The Extraction of Activation Parameters

While the measurement of activation parameters is conceptually simple, the actual process of extracting reliable values is quite difficult. The difficulties enumerated by Hirth and Nix with regard to dislocation motion (discussed in Sect. 2.1) have even more significant analogs in the studies of atomic-scale wear.

The first significant challenge is the correct identification of the stress state. In atomic-scale wear studies, the applied load is controlled as an input variable; the applied stress cannot be varied directly. Therefore, one must determine the location and values of the stress components that have the primary effect, and then find a model for calculating this stress from known variables. Park et al. [40] and Sheehan [41] both assumed that interfacial contact stresses are the most relevant, and rely on Hertzian contact mechanics to calculate values (though Sheehan includes an added adhesion force in the manner of the DMT model). However, it should be noted that the Hertz model assumes frictionless surfaces and small strains, both of which may be violated in adhesive contact involving a nanoscale asperity. Further, the Hertzian stresses apply in the absence of applied lateral force (implying, in this case, that wear would occur at the same rate for a stationary tip as for a sliding tip) and are based on continuum contact mechanics. While many nanoscale studies have fruitfully invoked continuum contact mechanics in the past, recent computer simulation work has demonstrated the breakdown of Hertzian behavior in nanoscale contacts under certain conditions [45, 46]. The Gotsmann and Bhaskaran studies [22, 27] propose that the interfacial shear stress has the most significant effect, yet still must rely on such models to calculate this stress from experimentally controllable parameters.

Adding to this first challenge of quantifying the stress state is the problem of uniformity across the contact. In the analysis of thermally activated processes, the system is treated as if it were comprised of a very large number of identical microscopic systems attempting the same transition. For a sliding tip, there are a large number of atoms that comprise the tip-sample contact and for realistic sliding times (minutes or even hours), there will be a very large number of "attempts." However, all atoms experience neither the same energy landscape nor the identical stress state [27]. With regard to energy landscape, consider the case of a single crystal tip with stepped edges (as proposed in [45]) sliding on a surface: atoms with a lower coordination number such as those at a step edge experience a very different energy landscape than atoms on the bottom surface of the tip with a higher coordination. This implies that wear of such a hypothetical single crystal tip would occur by loss of atoms from the step edges which recede. A

similar topic is specifically discussed in the work of Maw et al., where measurable wear is confined exclusively to the step edge [13]. In this case, an analysis of the wear rate would probe the activation parameters of the dissolution of atoms *in the step edges*. Alternatively, in experiments where the wearing surface is expected to be amorphous (e.g., a native silicon oxide), there is likely to be a distribution of coordination environments of surface atoms. Wear then would occur by the removal of atoms in the lowest coordination states and the wear process would result in a progressive change in the coordination state of any given surface atom until it is removed by wear. As such, an analysis of the wear rate would probe the activation parameters of the process of removing the most weakly bound atoms.

The distribution of stress in the contact zone is also an important consideration. The simplest assumption is that the constant stress equals the average value across the contact. A more accurate treatment would be to apply contact mechanics models to estimate the stress distribution within the contact. For example, for a Hertzian contact, the maximum value of the compressive stress is 1.5 times the average value. Similar deviations can be expected for the radial and shear stress components. It is important to note that due to the nonlinearity of the relation between stress and wear rate (Eqs. 7, 8), this modest variation in stress could result in a much larger variation in wear rate. For the case of tip wear, one could argue (as in Gotsmann and Lantz [22]) that the progression of tip shape as it is continuously worn will level out differences in stress. This, of course, only applies to the variation in a classical continuum-theory contact model. Such a treatment is not sufficient to describe variations at the atomic level, which are clearly relevant for atomic scale wear. For example, using molecular dynamics (MD) simulations of the contact between an amorphous spherical tip and an atomically flat single crystal surface, Luan and Robbins [45] have shown that the peak pressure acting on an individual atom in the tip can be up to 5–6 times the average value. Whatever assumptions are made about the state of stress under the tip, these variations in stress should be accounted for in any analysis based on transition state theory.

The second difficulty discussed in Sect. 2.1 is the changing local stress over the course of a test—even for a constant applied load. In Hirth and Nix [35], this referred to the fact that plastic flow altered the structure of the material and thus changed the local stress acting on the dislocation. In atomic-scale wear, even as the applied load is held constant, the modification that occurs due to wear of either the tip or surface means that the contact geometry is constantly changing, and thus the surface stresses are constantly changing. Of the three models described above, only Gotsmann [22] attempts to address this issue with in

situ pull-off tests to get a measure of tip radius in real time as the wear test is progressing.

The third difficulty discussed in Hirth and Nix is the assumptions about quantities that are not directly accessible. In plastic flow, this involves assuming that the pre-factor ($\dot{\varepsilon}_0$ in Eq. 3) is constant with respect to stress and temperature. The present studies on wear make similar assumptions about the pre-factor k_0 and, in addition, make even stronger assumptions about the form of the rate equation. In plastic flow studies, the activation volume is measured by plotting the logarithm of the rate of the process against the applied stress. As shown in Eq. 4, the slope of the plotted curve is a direct measurement of the activation volume. In contrast, the atomic-scale wear models assume a specific form of the work term ($\Delta W_{act} = \sigma \Delta V_{act}$) and further assume that the activation volume is constant with respect to stress (which it need not be, as discussed in [47] and [48]). Once these assumptions are made, the authors extract an activation volume by choosing the parameter that allows the best fit to the experimental data. If the assumptions are valid, then curve fitting should be an acceptable way to ascertain these values. However, these assumptions are not required if the activation volume is measured in the traditional, direct fashion.

The final difficulty in extracting activation parameters arises from the attempt to calculate activation energies (and thus enthalpies) with limited or no temperature variation. The activation enthalpy ΔH_{act} can be directly extracted by measuring the rate of wear at a variety of temperatures, as shown in Eq. 5. Sheehan's study varied temperature and reported an activation energy ΔU_{act} of 0.34 eV with a reported error of 50% due to the limited temperature variation. In Park et al., Gotsmann and Lantz, and Bhaskaran et al., an attempt is made to calculate the activation energy ΔU_{act} by assuming values for all other parameters in the wear rate equation and then solving for ΔU_{act}. However, values calculated in this fashion can depend strongly on the choice of parameters. The pre-factor k_0 is often assumed to be a lattice vibration frequency and is estimated as 10^{13}/s in Park et al. [40] and 10^{12}/s in Gotsmann and Lantz [22]. In Gotsmann and Lantz, there are additional constants: the reference velocity v_0 is taken as the sliding velocity of 1.5 mm/s (Gotsmann B, Lantz MA, Personal communication, 2010), the dimensionless pressure-dependence ξ was subsequently measured as 0.5 (Cannara R, Gotsmann B, Lantz MA, Unpublished results, 2007) and τ_0 does not need to be directly estimated as it is wrapped into the effective activation energy. Finally, and most significantly, a choice must be made for the form of ΔW_{act}—in particular, which stress does work on the system during the thermally activated event (Park et al. [40], Sheehan [41], and the two papers by Bhaskaran

et al. [27] and Gotsmann and Lantz [22] do not agree on the relevant stress component, as discussed in the previous subsection). Once this relevant stress is chosen, its value must be calculated as a function of controllable or measurable variables (applied load, material parameters, tip radius, etc.). This calculation depends on the model chosen to describe the contact (Hertz, one that includes adhesion, or a non-continuum simulation). Due to its presence in the exponential, errors in the calculation of the work term will be even more impactful than errors in the pre-factor. A direct measurement of the activation enthalpy according to Eq. 5 avoids the need for these assumptions.

Despite all of the aforementioned difficulties, four studies managed to extract activation parameters. And, as discussed earlier, it is impressive that the activation parameters all fall within reasonable bounds for atomic bond-breaking events.

3.4 The Interpretation of Activation Parameters

The interpretation of these experimentally measured values of activation parameters also differs among the various authors. In Park et al. [40], the authors assert that the activation volume is nearly equal to the volume of an ion in the calcite lattice and that the activation energy is comparable to the energy required for vacancy formation on a step edge. Such broad comparisons can be useful to ensure that measured values are of the right order of magnitude; however, in the Sheehan article, the activation volume is explicitly described as the volume removed per pass of the scanning probe. This interpretation is not consistent with transition state theory; in the context of the prototypical model shown in Fig. 6, the total worn volume describes the difference between state (a) and state (e), while the activation volume describes only the transition from state (b) to state (c). The Gotsmann study does not attribute the activation volume to any real space quantity, but compares the order of magnitude of activation parameters to quantities associated with bond breaking.

From a transition state theory perspective, the primary utility of activation parameters is as a signature of the underlying atomic-scale mechanism that underlies the macroscopic phenomenon. They allow for comparison among different sets of experiments and against theoretical values for the proposed underlying thermally activated reaction. Once a concrete picture of the atomic-mechanism of wear is proposed (along the lines of Fig. 6), then atomistic simulations of the process can be created to calculate expected values of the activation energy and activation volume. These expected values can be compared directly against measured values to provide further support for a thermally activated picture.

4 Suggested Future Work to Interrogate a Model Based on Transition State Theory

To address some of the remaining questions explored in Sect. 3, the following studies are recommended to allow an even deeper investigation of the fundamental origins of atomic-scale wear. Specifically, further experimental investigation is suggested into the effect of temperature on wear, stress, and velocity on atomic-scale wear. Also, a brief treatment of atomistic simulations of wear is presented along with past and future contributions to a better understanding of the science of atomic scale wear.

4.1 Experimentally Demonstrating the Effect of Temperature on Atomic-Scale Wear

As discussed, thermal activation is just one of many possible frameworks for describing wear at the atomic scale. Decisively establishing this description as the correct one requires experimental evidence demonstrating an Arrhenius dependence of the rate of atom transfer on inverse temperature. Ideally a wear study of this kind would vary temperature over several orders of magnitude as has been done with plastic flow, as described in Sect. 2.1.

Unfortunately, a detailed temperature study is challenging for a variety of reasons. Aside from the experimental difficulty of heating or cooling the tip-sample contact, the analysis will be complicated by the temperature dependence of other parameters, especially friction. The temperature dependence of friction can be substantial [49, 50] and even non-monotonic [51, 52] and thus will significantly alter the shear stresses acting at the interface. In addition, a large enough increase in temperature will cause softening of the mechanical properties of the tip/ sample materials, thus altering the geometry and stresses of the contact. Therefore, such a temperature study would ideally measure friction and wear concurrently, or be performed on a system where the temperature dependence of friction and mechanical properties is not strong, or has been determined previously such as for a silicon tip sliding over Si, SiO_2, SiC, or NaCl [49–53].

There is further no guarantee that the activation volume itself is constant with temperature (as discussed in [47]) so it would be useful to have a comprehensive analysis that performs a study similar to Park et al. [40] or Gotsmann and Lantz [22] *at each temperature*. Finally, the pre-factor (f in Eq. 1 or k_0 in Eq. 6, designated the *attempt frequency* above) may vary with temperature. Depending on dissipative processes active when the system moves along the lowest energy path (Fig. 2), f can increase or decrease with increasing temperature [31].

It would be difficult for all of the above effects to be addressed in a single study of atomic scale wear. Rather, these points are suggested as guidelines for the design of new experiments, and for the analysis of the body of wear data as it develops, especially with regard to temperature.

4.2 Determining Which is the Primary "Activating Stress" for Atomic-Scale Wear

The free energy of activation, ΔG_{act}, is reduced when an applied stress does work during the thermally activated transition. However, each of the above models assumes that a different stress does work during the transition: the Park et al. study uses the Hertzian radial stress in its calculation, Sheehan uses the Hertzian shear stress at the interface, and Gotsmann and Lantz use the interfacial shear stress induced by sliding friction. It is crucial to determine which of these stresses is primarily involved in wear for accurate data analysis.

In principle, it should be possible to distinguish which stress does work (and thus which is the *activating stress*) through further study of the dependence of wear on the applied load F_N. Specifically, in Park et al. and in Sheehan, Hertzian stresses, which are present in static contact and depend only on mechanical properties of the materials and the shape of the tip, have a dependence of $F_N^{1/3}$ [54]. In contrast, the Gotsmann and Lantz picture assumes that the activation barrier depends primarily on the shear stress acting on the surface atoms due to frictional sliding. At a constant velocity, this interfacial shear stress τ is usually approximated with a linear dependence on pressure [55]:

$$\tau = \tau_0 + \xi P, \tag{9}$$

where τ_0 is the constant part of the shear stress and P is the mean normal contact pressure. According to multiple AFM studies, the constant ξ, describing the pressure dependence, is typically in the range of 10^{-3}–10^{-1} depending on the materials in contact [55]. In Gotsmann and Lantz, this pressure dependence is responsible for an observed slowing down of the wear rate as the tip gets blunter and surface stresses are reduced, diminishing the stress-induced reduction of the energy barrier.

Intuitively, either the shear or tensile component of stress should be most relevant for facilitating bond rupture and atom removal or displacement. If so, then one of these stresses would affect the free energy of activation ΔG_{act} and thus would appear in the exponential term of the Arrhenius-type equation. However, more experimental evidence is required to firmly establish the most relevant component for any given experimental arrangement. In addition, atomistic, MD, or other computer simulation techniques may prove useful in modeling proposed reactions and determining the impact of different stress components, as discussed in the following sections.

4.3 Disentangling the effect of velocity on atomic-scale wear

The underlying equation of a thermally activated picture of atomic-scale wear (Eq. 6) is independent of velocity. Therefore, if the shear stress does not enter into the free energy of activation (as assumed by Park et al., Sheehan, and Kopta and Salmeron), or if the shear stress does not depend on velocity (as in the description from [56]) then the rate of wear is independent of tip velocity. The only predicted effect of sliding speed in these models is to change the amount of time in contact for a given sliding distance. Thus, the rate of successful atom transfers per second will be unchanged, but the amount of wear observed for a given sliding distance will scale linearly with contact time and thus inversely with sliding velocity.

The effect of velocity in the Gotsmann and Lantz picture is more complex because the activation free energy depends on the applied interfacial shear stress, which in turn is assumed to depend on sliding velocity. This is based on multiple experimental observations of velocity effects as well as theoretical models which predict such a dependence, including the Prandtl–Tomlinson model. This frictional shear stress has itself been described as a thermally activated process in models of single-asperity interfacial friction whereby the tip slides in quasi-static equilibrium along the corrugated energy surface representing the sample [55]. The latter is captured in the Briscoe and Evans equation expressing the shear stress applied to an interface due to sliding friction [42]:

$$\tau = \tau_0 + \xi P + \left(\frac{k_B T}{\Delta V_{act}^{friction}}\right) \ln\left(\frac{v}{v_0}\right). \tag{10}$$

Although this equation was originally derived for organic thin films [42], it has been shown to be applicable to a variety of tip-sample systems and to stick–slip motion as derived from the Prandtl–Tomlinson model [57–60].

Equation 10 for the interfacial shear stress was applied in Gotsmann and Lantz [22] to the wear problem. In that picture, the formula for the rate of change of tip height (which is proportional to the rate of atom loss, by geometrical arguments) is as follows:

$$\frac{\partial h(t)}{\partial t} = bk_{atom-loss} = bk_0 \exp\left(-\frac{\Delta U_{act} - \tau \Delta V_{act}}{k_B T}\right) \tag{11}$$

In Gotsmann and Lantz, it is assumed that the shear stress has the form given in Eq. 10 and it is further assumed that the activation volumes for the friction and wear processes are equal. In this case, terms cancel neatly, leaving a differential equation for the rate of height loss *per sliding distance* (rather than per second) which is wholly independent of sliding velocity (Eq. 4 in [22]).

The velocity dependence can be examined under the limits of other assumptions. First, Eq. 10 represents only one limiting case and, for smaller scanning speeds, one should instead use a velocity-dependent term in the exponential part of Eq. 11 of the form [61]:

$$\tau \propto \text{const} + \ln\left(\frac{v}{v_0}\right)^{2/3} \tag{12}$$

In this limit, the exponent and natural log terms still cancel, but there is a $v^{2/3}$ term that remains in the final wear rate equation. In addition, if the activation parameters of friction are *not* assumed equal to those of atom rupture, then account must be taken of each. With these modified assumptions, the differential equation from the Gotsmann and Lantz paper would take the form (without explicitly spelling out all temperature dependence):

$$\frac{\partial r(d)}{\partial d} = \tan(\theta)\frac{k_0 b}{v_0}\left(\frac{v}{v_0}\right)^{\left(1.5\frac{\Delta V_{act}^{wear}}{\Delta V_{act}^{friction}}-1\right)}$$
$$\times \exp\left(-\frac{(\Delta U_{act} - \Delta V_{act}^{wear}\tau_0)}{k_B T} + \frac{\Delta V_{act}^{wear}\xi P}{k_B T}\right). \tag{13}$$

The Gotsmann and Lantz article acknowledges the intertwined nature of friction and wear by extracting compound fit parameters that describe the action of both processes concurrently [22].

In total, the wear rate per sliding distance could be independent of velocity, could vary as velocity to the power of ½, or could have some other arbitrary dependence (determined by the ratio of activation volumes). Therefore, a combined, systematic study of the velocity dependence of friction and wear could shed light on this question. Concurrent measurements of the frictional force, combined with knowledge of tip shape, would permit the direct calculation of the shear strength, circumventing the need for an assumed form of τ and allowing an evaluation of previous assumptions.

It should be noted, however, that varying the time or velocity scale in experiments to uncover the underlying kinetics ideally requires variation over several orders of magnitude. Especially with exponential equations, false trends can be easily detected with insufficient variation. However, experimentally this may be difficult to accomplish with many AFM systems. For the case of atomic-scale wear, the wear rates can be so low that high scanning speeds and long duration experiments are required to accurately measure the wear rate. For example, in the work of Gotsmann and Lantz, a sliding velocity of 1.5 mm/s in combination with sliding times of up to 1 week were required to quantify low-load wear. Acquiring the same amount of data at a significantly lower sliding velocity is unfeasible.

4.4 Using Atomistic Simulations to Elucidate Atomic-Scale Wear

A key complement to the above-mentioned experimental work will be computer simulations based on MD and ab initio techniques. Already, there is a developing body of literature where these techniques are used to characterize the contact area and stresses (normal and frictional) of a nanoscale contact (for example, [45, 46, 62]). Some of these models have even been extended to model certain aspects of wear. For instance, in a study on the adhesive loads associated with atomically sharp diamond tips, Jarvis et al. [63] slide the tip along the surface and find that the contacting atom is removed from the tip after just 1.6 Å of sliding. Further, Harrison and Brenner use MD models to slide two diamond surfaces past one another and find that wear initiates by the removal of hydrogen from the H-terminated surfaces and continues by radical recombination, transient surface adhesion, and debris formation [64]. Other studies use MD to model the sliding of atomically flat surfaces in intimate contact and demonstrate plastic deformation and mechanical mixing of the surface material [65, 66].

There has not yet been an atomistic simulation of wear in the context of transition state theory. A full treatment of the details of such a simulation is beyond the scope of this article. Yet, it can be imagined to follow the style of earlier work modeling the stress-dependent hydrolysis of silica in water [67]. In this work, Zhu et al. use molecular orbital theory and the nudged elastic band (NEB) technique to find the minimum energy path along the potential energy surface, giving a direct measurement of the predicted activation energy for the proposed reaction. Not only are the authors able to predict the dependence of activation barrier on stress, but also they go even further to show that different reaction pathways can be thermodynamically favorable at different stresses and that, when the stress is high enough, a given pathway may no longer require thermal activation to overcome the barrier.

Overall, simulation techniques make possible: the elimination of certain assumptions, such as the applicability of continuum mechanics; the study of wear under conditions that are difficult or impossible to access experimentally; and the creation of testable predictions that can be directly compared with experimental results. It seems likely that atomistic simulations will be critical to solving many of the questions raised in this article.

5 Conclusions

This article has reviewed recent atomic-scale wear studies in light of formal transition state theory. The primary conclusions are as follows:

(1) Substantial experimental evidence demonstrates that atomic-scale wear occurs at single-asperity contacts for a variety of materials, highlighting the need to understand this process more deeply.

(2) Many of the previous analyses of these experiments used equations taken from transition state theory, but did not fully address the physics behind such a model. Specifically, the analysis should specify: the atomic-scale transition which is proposed to be thermally activated; the configuration of the system in its initial, activated, and final states; and the assumptions made about the tip-sample system such that the requirements of transition state theory are satisfied and Boltzmann statistics can be applied.

(3) The method of measurement and the physical interpretation of activation parameters vary widely from author to author. In particular, while various studies measured activation volumes directly, the values obtained depended on which stress component was chosen as the activating stress and how this component was calculated. Also, reported values of activation energy were often not measured in the typical manner of transition state theory (i.e., measuring the slope of the data as presented on an Arrhenius plot) and thus have high degrees of uncertainty. In addition, various authors offer differing interpretations of the physical meaning of measured values—some of which are demonstrably incorrect.

(4) Further experimental work is required to confirm and interrogate models based on transition state theory. First, studies over a range of temperatures would be ideal to verify the Arrhenius dependence of wear rate on temperature, which is the hallmark of a thermally activated process. These studies would also allow the direct extraction of the activation energy. Second, measuring the dependence of wear on applied load would help determine which stress component has the strongest impact (normal or shear stresses arising from contact mechanics, or shear stresses due to interfacial friction). Finally, a concurrent investigation of the velocity dependence of both atomic-scale wear and friction will allow further elucidation of the effect of different stresses and may help disentangle these interrelated phenomena. With such approaches in hand, new insights into the mechanisms of wear for a wide array of materials can be developed, possibly even with predictive potential. Such knowledge would be tremendously beneficial, as it could be applied to rationally selecting materials, conditions, and design parameters for applications where tribological contact occurs, including atomic force microscopy, probe-based nanomanufacturing and data storage, and NEMS devices.

References

1. de Boer, M.P., Mayer, T.M.: Tribology of MEMS. MRS Bull. **26**, 302–304 (2001)
2. Romig Jr., A.D., Dugger, M.T., McWhorter, P.J.: Materials issues in microelectromechanical devices: science, engineering, manufacturability and reliability. Acta Mater. **51**, 5837–5866 (2003)
3. Maboudian, R., Ashurst, W.R., Carraro, C.: Tribological challenges in micromechanical systems. Tribol. Lett. **12**, 95–100 (2002)
4. Xu, S., Amro, N.A., Liu, G.Y.: Characterization of AFM tips using nanografting. Appl. Surf. Sci. **175**, 649–655 (2001)
5. Cruchon-Dupeyrat, S., Porthun, S., Liu, G.Y.: Nanofabrication using computer-assisted design and automated vector-scanning probe lithography. Appl. Surf. Sci. **175**, 636–642 (2001)
6. Lieber, C.M., Kim, Y.: Nanomachining and manipulation with the atomic force microscope. Adv. Mater. **5**, 392–394 (1993)
7. Vettiger, P., Cross, G., et al.: The 'Millipede'—nanotechnology entering data storage. IEEE Trans. Nanotechnol. **1**, 39–55 (2002)
8. Szlufarska, I., Chandross, M., Carpick, R.W.: Recent advances in single-asperity nanotribology. J. Phys. D **41**, 123001 (2008)
9. Meyer, E., Hug, H.J., Bennewitz, R.: Scanning Probe Microscopy: The Lab on a Tip. Springer, New York (2003)
10. Khurshudov, A.G., Kato, K., Koide, H.: Nano-wear of the diamond AFM probing tip under scratching of silicon, studied by AFM. Tribol. Lett. **2**, 345–354 (1996)
11. Bloo, M.L., Haitjema, H., Pril, W.O.: Deformation and wear of pyramidal, silicon-nitride AFM tips scanning micrometre-size features in contact mode. Measurement **25**, 203–211 (1999)
12. Zhao, Q.L., Dong, S., Sun, T.: Investigation of an atomic force microscope diamond tip wear in micro/nano-machining. Key Eng. Mat. **202–203**, 315–320 (2001)
13. Maw, W., Stevens, F., et al.: Single asperity tribochemical wear of silicon nitride studied by atomic force microscopy. J. Appl. Phys. **92**, 5103–5109 (2002)
14. D'Acunto, M.: Theoretical approach for the quantification of wear mechanisms on the nanoscale. Nanotechnology **15**, 795–801 (2004)
15. Chung, K.-H., Lee, Y.-H., Kim, D.-E.: Characteristics of fracture during the approach process and wear mechanism of a silicon AFM tip. Ultramicroscopy **102**, 161–171 (2005)
16. Liu, H., Klonowski, M., et al.: Advanced atomic force microscopy probes: wear resistant designs. J. Vac. Sci. Technol. B **23**, 3090–3093 (2005)
17. Tao, Z., Bhushan, B.: Surface modification of AFM silicon probes for adhesion and wear reduction. Tribol. Lett. **21**, 1–16 (2006)
18. Bhaskaran, H., Sebastian, A., Despont, M.: Nanoscale PtSi tips for conducting probe technologies. IEEE Trans. Nanotechnol. **8**, 128–131 (2009)
19. Kopycinska-Mueller, M., Geiss, R.H., Hurley, D.C.: Size-related plasticity effects in AFM silicon cantilever tips. Mater. Res. Soc. Symp. Proc. **924**, 19–24 (2006)
20. Chung, K.H., Kim, D.E.: Fundamental investigation of micro wear rate using an atomic force microscope. Tribol. Lett. **15**, 135–144 (2003)
21. Tao, Z.H., Bhushan, B.: Surface modification of AFM Si_3N_4 probes for adhesion/friction reduction and imaging improvement. Trans. ASME **128**, 865–875 (2006)
22. Gotsmann, B., Lantz, M.A.: Atomistic wear in a single asperity sliding contact. Phys. Rev. Lett. **101**, 125501 (2008)
23. Bhushan, B., Kwak, K.J.: Velocity dependence of nanoscale wear in atomic force microscopy. Appl. Phys. Lett. **91**, 3 (2007)
24. Kopta, S., Salmeron, M.: The atomic scale origin of wear on mica and its contribution to friction. J. Chem. Phys. **113**, 8249–8252 (2000)
25. Agrawal, R., Moldovan, N., Espinosa, H.D.: An energy-based model to predict wear in nanocrystalline diamond atomic force microscopy tips. J. Appl. Phys. **106**, 064311 (2009)
26. Gnecco, E., Bennewitz, R., Meyer, E.: Abrasive wear on the atomic scale. Phys. Rev. Lett. **88**, 215501 (2002)
27. Bhaskaran, H., Gotsmann, B., et al.: Ultralow nanoscale wear through atom-by-atom attrition in silicon-containing diamond-like carbon. Nat. Nanotechnol. **5**, 181–185 (2010)
28. Liu, J., Grierson, D.S., et al.: Preventing nanoscale wear of atomic force microscopy tips through the use of monolithic ultrananocrystalline diamond probes. Small **6**, 1140–1149 (2010)
29. Christian, J.W.: The Theory of Transformations in Metals and Alloys. Pergamon, Oxford (2002)
30. Vineyard, G.H.: Frequency factors and isotope effects in solid state rate processes. J. Phys. Chem. Solids **3**, 121–127 (1957)
31. Hanggi, P., Talkner, P., Borkovec, M.: Reaction-rate theory—50 years after Kramers. Rev. Mod. Phys. **62**, 251–341 (1990)
32. Kauzmann, W.: Flow of solid metals from the standpoint of chemical-rate theory. Trans. AIME **143**, 57–83 (1941)
33. Rohde, R.W., Pitt, C.H.: Dislocation velocities in nickel single crystals. J. Appl. Phys. **38**, 876–879 (1967)
34. Gibbs, G.B.: Thermodynamics of thermally-activated dislocation glide. Phys. Status Solidi **10**, 507–512 (1965)
35. Hirth, J.P., Nix, W.D.: An analysis of thermodynamics of dislocation glide. Phys. Status Solidi **35**, 177–188 (1969)
36. Kocks, U.F., Argon, A.S., Ashby, M.F.: Thermodynamics and kinetics of slip. Prog. Mater. Sci. **19**, 1–281 (1975)
37. Taylor, G.: Thermally-activated deformation of BCC metals and alloys. Prog. Mater. Sci. **36**, 29–61 (1992)
38. Gibbs, G.B.: On interpretation of experimental activation parameters for dislocation glide. Phil. Mag. **20**, 867–872 (1969)
39. Hull, D., Bacon, D.J.: Introduction to Dislocations, 4th edn. Butterworth-Heinemann, Oxford (1984)
40. Park, N.S., Kim, M.W., et al.: Atomic layer wear of single-crystal calcite in aqueous solution scanning force microscopy. J. Appl. Phys. **80**, 2680–2686 (1996)
41. Sheehan, P.E.: The wear kinetics of NaCl under dry nitrogen and at low humidities. Chem. Phys. Lett. **410**, 151–155 (2005)
42. Briscoe, B.J., Evans, D.C.B.: The shear properties of Langmuir-Blodgett Layers. Proc. R. Soc. Lond. A **380**, 389–407 (1982)
43. Helt, J.M., Batteas, J.D.: Wear of mica under aqueous environments: direct observation of defect nucleation by AFM. Langmuir **21**, 633–639 (2005)
44. Hong, U.S., Jung, S.L., et al.: Wear mechanism of multiphase friction materials with different phenolic resin matrices. Wear **266**, 739–744 (2009)
45. Luan, B., Robbins, M.O.: The breakdown of continuum models for mechanical contacts. Nature **435**, 929–932 (2005)
46. Mo, Y.F., Turner, K.T., Szlufarska, I.: Friction laws at the nanoscale. Nature **457**, 1116–1119 (2009)
47. Krausz, A.S., Eyring, H.: Deformation Kinetics. Wiley, New York (1975)
48. Li, J.: The mechanics and physics of defect nucleation. MRS Bull. **32**, 151–159 (2007)
49. Zhao, X.Y., Hamilton, M., et al.: Thermally activated friction. Tribol. Lett. **27**, 113–117 (2007)
50. Zhao, X., Phillpot, S.R. et al.: Transition from thermal to athermal friction under cryogenic conditions. Phys. Rev. Lett. **102**, 1861021–1861024 (2009)

51. Jansen, L., Schirmeisen, A., et al.: Nanoscale frictional dissipation into shear-stressed polymer relaxations. Phys. Rev. Lett. **102**, 4 (2009)

52. Schirmeisen, A., Jansen, L., et al.: Temperature dependence of point contact friction on silicon. Appl. Phys. Lett. **88**, 123108 (2006)

53. Barel, I., Urbakh, M., et al.: Multibond dynamics of nanoscale friction: the role of temperature. Phys. Rev. Lett. **104**, 066104 (2010)

54. Johnson, K.L.: Contact Mechanics. University Press, Cambridge (1987)

55. Carpick, R.W., Salmeron, M.: Scratching the surface: fundamental investigations of tribology with atomic force microscopy. Chem. Rev. **97**, 1163–1194 (1997)

56. Zworner, O., Holscher, H., et al.: The velocity dependence of frictional forces in point-contact friction. Appl. Phys. A **66**, S263–S267 (1998)

57. Riedo, E., Gnecco, E., et al.: Interaction potential and hopping dynamics governing sliding friction. Phys. Rev. Lett. **91**, 84502 (2003)

58. Bouhacina, T., Aimé, J.P., et al.: Tribological behaviour of a polymer grafted in silanized silica probed with a nanotip. Phys. Rev. B **56**, 7694–7703 (1997)

59. Gnecco, E., Bennewitz, R., et al.: Velocity dependence of atomic friction. Phys. Rev. Lett. **84**, 1172–1175 (2000)

60. Chen, J., Ratera, I., et al.: Velocity dependence of friction and hydrogen bonding effects. Phys. Rev. Lett. **96**, 4 (2006)

61. Yi, S., Dube, M., Grant, M.: Thermal effects on atomic friction. Phys. Rev. Lett. **87**, 174301 (2001)

62. Gao, G.T., Mikulski, P.T., Harrison, J.A.: Molecular-scale tribology of amorphous carbon coatings: effects of film thickness, adhesion, and long-range interactions. J. Am. Chem. Soc. **124**, 7202–7209 (2002)

63. Jarvis, M.R., Perez, R., Payne, M.C.: Can atomic force microscopy achieve atomic resolution in contact mode? Phys. Rev. Lett. **86**, 1287–1290 (2001)

64. Harrison, J.A., Brenner, D.W.: Simulated tribochemistry—an atomic-scale view of the wear of diamond. J. Am. Chem. Soc. **116**, 10399–10402 (1994)

65. Kim, H.J., Karthikeyan, S., Rigney, D.: A simulation study of the mixing, atomic flow and velocity profiles of crystalline materials during sliding. Wear **267**, 1130–1136 (2009)

66. Rigney, D.A., Fu, X.Y., et al.: Examples of structural evolution during sliding and shear of ductile materials. Scr. Mater. **49**, 977–983 (2003)

67. Zhu, T., Li, J., et al.: Stress-dependent molecular pathways of silica-water reaction. J. Mech. Phys. Sol. **53**, 1597–1623 (2005)

68. Zhu, T., Li, J., et al.: Temperature and strain-rate dependence of surface dislocation nucleation. Phys. Rev. Lett. **100**, 4 (2008)

69. Crawford, J.H., Slifkin, L.M.: Point Defects in Solids. Plenum Publishing, New York (1972)

70. Liu, J., Notbohm, J.K. et al.: Method for characterizing nanoscale wear of atomic force microscope tips. ACS Nano (2010). doi: 10.1021/nn100246g